ORIGINAL RESEARCH

Tollip Negatively Regulates Vascular Smooth Muscle Cell–Mediated Neointima Formation by Suppressing Akt-Dependent Signaling

Hong Zhi, MD, PhD; Fu-Han Gong, MD; Wen-Lin Cheng, MD; Kongbo Zhu, MD; Long Chen, MD; Yuyu Yao, MD; Xingzhou Ye, MD; Xue-Yong Zhu, BS; Hongliang Li, MD, PhD

***Background*—**Tollip, a well-established endogenous modulator of Toll-like receptor signaling, is involved in cardiovascular diseases. The aim of this study was to investigate the role of Tollip in neointima formation and its associated mechanisms.

***Methods and Results*—**In this study, transient increases in Tollip expression were observed in platelet-derived growth factor-BB–treated vascular smooth muscle cells and following vascular injury in mice. We then applied loss-of-function and gain-of-function approaches to elucidate the effects of Tollip on neointima formation. While exaggerated neointima formation was observed in Tollip-deficient murine neointima formation models, Tollip overexpression alleviated vascular injury–induced neointima formation by preventing vascular smooth muscle cell proliferation, dedifferentiation, and migration. Mechanistically, we demonstrated that Tollip overexpression may exert a protective role in the vasculature by suppressing Akt-dependent signaling, which was further confirmed in rescue experiments using the Akt-specific inhibitor (AKTI).

***Conclusions*—**Our findings indicate that Tollip protects against neointima formation by negatively regulating vascular smooth muscle cell proliferation, dedifferentiation, and migration in an Akt-dependent manner. Upregulation of Tollip may be a promising strategy for treating vascular remodeling–related diseases. **(*J Am Heart Assoc*. 2018;7:e006851. DOI: 10.1161/JAHA.117.006851.)**

Key Words: differentiation • migration • neointima formation • proliferation • Tollip • vascular smooth muscle

Arteriosclerotic cardiovascular disease is a leading cause of mortality and morbidity in developed nations.[1] Although revascularization therapy, including angioplasty, stenting, atherectomy, and bypass surgery, is widely accepted as the standard treatment, mechanical injuries to arteries during these surgical procedures appear inevitable and lead to a gradual re-narrowing of arteries because of neointima formation.[2] Vascular smooth muscle cells (VSMCs) play important roles in the pathogenesis of neointima formation.[3,4] During surgical revascularization, the integrity of the endothelium may be damaged by mechanical injuries and result in the infiltration of inflammatory cells. Both dysfunctional endothelial cells and inflammatory cells synthesize and secrete various cytokines and growth factors, especially platelet-derived growth factor (PDGF), which facilitates the switch of VSMCs from a contractile phenotype to a synthetic phenotype.[5] Subsequently, the synthetic VSMCs, which express decreased levels of adult smooth muscle–specific proteins, migrate from the media into the intimal layer and proliferate to form neointimal lesions.[6] Therefore, in-depth investigations that may reveal the underlying mechanisms of intimal hyperplasia are required for developing novel treatments that prevent vessel restenosis after revascularization therapy.

The Toll-interacting protein (Tollip), which contains a Tom1 binding domain at the N-terminus, a conserved 2 domain at the center, and a coupling ubiquitin to endoplasmic reticulum degradation domain at the C-terminus, was identified as a critical endogenous modulator of Toll-like receptor (TLR) signaling-mediated immune responses.[7] Furthermore, recent evidence has revealed that Tollip is involved in cardiovascular diseases, including cardiac remodeling after chronic pressure overload and myocardial infarction.[8–10] Tollip can physically

From the Department of Cardiology, Zhongda Hospital Affiliated to Southeast University, Nanjing, China (H.Z., K.Z., L.C., Y.Y., X.Y.); Department of Cardiology, Renmin Hospital of Wuhan University, Wuhan, China (F.-H.G., W.-L.C., X.-Y.Z., H.L.); Basic Medical School, Wuhan University, Wuhan, China (F.-H.G., W.-L.C., X.-Y.Z., H.L.); Institute of Model Animal of Wuhan University, Wuhan, China (F.-H.G., W.-L.C., X.-Y.Z., H.L.).

Accompanying Tables S1 through S3 and Figures S1 through S4 are available at http://jaha.ahajournals.org/content/7/12/e006851/DC1/embed/inline-supplementary-material-1.pdf

Correspondence to: Hong Zhi, MD, PhD, Department of Cardiology, Zhongda Hospital Affiliated to Southeast University, No. 87 Dingjiaqiao, Gulou District, Nanjing 210009, China. E-mail: zhihongnj@163.com
Hongliang Li, MD, PhD, Department of Cardiology, Renmin Hospital of Wuhan University, Basic Medical School, Institute of Model Animal of Wuhan University, Luojia Mount Wuchang, Wuhan 430072, China. E-mail: lihl@whu.edu.cn

Received June 6, 2017; accepted November 16, 2017.

Clinical Perspective

What Is New?

- Previously, the precise role of Tollip in neointima formation has not been well addressed.
- This study provides the first evidence that Tollip protects against neointima formation by negatively regulating vascular smooth muscle cell proliferation, dedifferentiation, and migration in an Akt-dependent manner.

What Are the Clinical Implications?

- A gradual re-narrowing of arteries because of neointima formation limited the efficiency of revascularization therapy in arteriosclerotic cardiovascular disease.
- Upregulation of Tollip may be a potential therapeutic strategy for treating vascular injury–induced neointima formation.

associate with TLR2 and TLR4 to suppress TLR signaling.[11] TLR2 participates in *Chlamydia pneumoniae* infection–mediated VSMC migration.[12] In addition, Graaf and colleagues demonstrated that heat shock protein 60–induced activation of TLR2 and TLR4 could contribute to VSMC proliferation.[13] Therefore, we speculate that Tollip has potential regulatory effects on neointima formation, which is a complicated vascular pathological procedure interfering with VSMC phenotypic switching, migration, and proliferation.

To test our hypothesis, global Tollip-knockout (Tollip-KO) mice and SMC-specific Tollip transgenic (Tollip-TG) mice were generated to explore the effects of Tollip on VSMC dedifferentiation, migration, and proliferation in response to vascular injury. In addition, the protective role of Tollip in neointima formation was further verified in a Tollip-KO rat strain. Mechanistically, signaling assays suggest that Tollip suppresses neointima formation by inhibiting Akt-dependent signaling, which was further confirmed by a rescue experiment using an Akt-specific inhibitor (AKTI). Based on our findings, Tollip upregulation is a potential therapeutic strategy for treating vascular injury–induced neointima formation.

Materials and Methods

The data, analytic methods, and study materials will be made available upon request to other researchers for purposes of reproducing the results or replicating the procedure.

Human Artery Samples

All procedures related to human samples complied with the principles of the Declaration of Helsinki and were approved by the ethics committee of the Zhongda Hospital of Southeast University in Nanjing, China. The human artery samples were obtained from patients at the Zhongda Hospital of Southeast University in Nanjing, China. We acquired informed consent from the participating patients. The in-stent restenotic arteries were obtained from diseased femoral arteries that were removed during artery bypass grafting (n=3). The control arteries were acquired from normal regions of the femoral arteries from patients who underwent bypass grafting because of lower limb arteriosclerosis obliterans (n=3).

Study Animals

All animal experiments complied with the *National Institutes of Health Guide for the Care and Use of Laboratory Animals*. The investigation was approved by the Animal Care and Use Committee of the Zhongda Hospital of Southeast University.

To establish the Tollip-TG mice, full-length human Tollip cDNA was amplified by the primers 5′-CCGGAATTCATGGCGACCACCGTCAGC-3′ (forward) and 5′-CCGGAATTCGGACTCTTCACCCATTTGCAGC-3′ (reverse). Subsequently, the full-length human Tollip cDNA was cloned into the SMC-specific TG vector containing a mouse SM22α promoter, a 50-HA tag, and an SV40 polyA signal. The construct was then microinjected into fertilized C57BL/6J embryos. The successful generation of Tollip transgenic mice was confirmed with polymerase chain reaction (PCR) and Western blotting. The Tollip-TG mice were identified using the primers 5′-CC TTCCAGTCCACAAACGAC-3′ and 5′-ATCATGCCCTCCTTGTC ATC-3′. The generation of the Tollip-KO mice and the Tollip-KO rats was described previously.[9,10]

Specific AKT Inhibitor IV (AKTI, 0.5 mg/kg per day, SC-203809, Santa Cruz Biotechnology) was intraperitoneally injected every 3 days from 1 week before surgery to 4 weeks after the operation. The control littermates were administered the same volume of PBS.

Murine Neointima Formation Model

The mouse neointima formation model was generated by carotid artery wire injury in the left carotid artery (LCA). First, 8- to 10-week-old mice with body weights of 24 to 27 g were anesthetized with sodium pentobarbital (50 mg/kg, intraperitoneally, Sigma). After local analgesia via the subcutaneous injection of 1% lidocaine hydrochloride, the LCA of the mouse was exposed by blunt dissection. Then, the external carotid artery was ligated near the bifurcation with an 8-0 suture. The common and internal carotid arteries were clamped to interrupt blood flow. A transverse incision was made proximal to the suture in the external carotid artery. A guidewire (No. C-SF-15-15; Cook) was subsequently introduced into the arterial lumen toward the aortic arch and withdrawn with rotation 5 times.

After successful vascular injury, the guidewire and vascular clamps were sequentially removed from the arterial lumen. Finally, the skin incision was closed. By contrast, sham-operated controls were subjected to a similar surgical procedure without the incision or injury in their left carotid arteries. Tissue samples were collected for morphological and biochemical assays at the indicated time points after surgery.

The carotid artery balloon injury model was established in male SD rats (≈300 g in weight). In brief, after anesthetization, the left external carotid artery of the rat was exposed, and 30 IU heparin was injected through the external jugular vein. After a transverse incision was performed in the external carotid artery, a Fogarty 2F catheter (Baxter) was introduced into the arterial lumen toward the common carotid artery. The catheter was then inflated with 0.2 to 0.25 mL of saline and withdrawn with rotation 10 times. All operations were performed by a single surgeon.

Murine Grouping

Murine study contains 16 groups: WT/sham (n=16), Tollip-KO/sham (n=16), WT/vascular injury (n=17), Tollip-KO/vascular injury (n=16), nontransgenic (NTG)/sham (n=16), Tollip-TG/sham (n=16), NTG/vascular injury (n=16), Tollip-TG/vascular injury (n=16), WT/PBS/vascular injury (n=12), WT/AKTI/vascular injury (n=12), Tollip-KO/PBS/vascular injury (n=12), Tollip-KO/AKTI/vascular injury (n=12), SD-control/sham (n=10), SD-Tollip-KO/sham (n=10), SD-control/vascular injury (n=10), and SD-Tollip-KO/vascular injury (n=10).

Histological Analysis

The mice were euthanized by an intraperitoneal injection of sodium pentobarbital (150 mg/kg) at 0, 7, 14, or 28 days postoperation. The carotid arteries were collected after perfusion, fixed with 4% paraformaldehyde, and embedded in paraffin. The bifurcation site of the LCA was then sliced into a series of cross-sections (3–5 μm thick). In addition, the sections were stained with elastica van Gieson staining for morphometric analysis. The extent of neointima formation was evaluated as the intimal area and the ratio of the intima to media (I/M), which were determined with Image-Pro Plus software (version 6.0) by a single observer who was blinded to the experimental protocols. A mean value was calculated from more than 5 different sections of each artery sample.

For immunofluorescence staining, the carotid artery sections were subjected to an antigen retrieval process for 5 minutes. The sections were then treated with 10% goat serum and were incubated overnight with specific primary antibodies at 4°C. The primary antibodies (Table S1) included rabbit anti-proliferating cell nuclear antigen (PCNA) (ab92552; Abcam), mouse anti-α-smooth muscle actin (SMA) (ab7817; Abcam), rabbit anti-cyclinD1 (#2978; Cell Signaling Technology), rabbit anti-SM22α (ab14106; Abcam), rabbit anti-smoothelin (sc28562; Santa Cruz), and rabbit anti-Tollip (ab37155; Abcam). The sections were then washed using PBS and treated with the corresponding secondary antibodies for 1 hour at 37°C. The secondary antibodies included Alexa Fluor 488-conjugated goat anti-mouse IgG (A11001; Invitrogen), Alexa Fluor 488-conjugated goat anti-rabbit IgG (A11008; Invitrogen), and Alexa Fluor 568-conjugated goat anti-rabbit IgG (A11011; Invitrogen). Then, 4′,6-diamidino-2-phenylindole was utilized to stain the nuclei. Images were obtained with a fluorescence microscope (Olympus DX51) and DP2-BSW software (version 2.2). The integrated optical density values were calculated with Image-Pro Plus software (version 6.0) by a single operator who was blinded to the experimental protocol.

Cultured VSMCs

Human aortic smooth muscle cells were purchased from the American Type Culture Collection. Primary VSMCs were separated and purified from the thoracic aortas of C57BL/6 mice, Tollip-KO mice, SMC-Tollip-TG mice, and SD rats via enzymatic digestion. The VSMCs were then cultured in Dulbecco's modified Eagle's medium/F12 supplemented with 1% penicillin-streptomycin and 10% fetal bovine serum (SV30087.02, HyClone) in a 5% CO_2 incubator at 37°C. Cells that were at least 3 passages old were utilized in the following experiments.

Migration Assay

Modified Boyden chambers were utilized to assess the extent of VSMC migration. First, VSMCs from murine arteries were isolated and washed. After the VSMCs were resuspended, $\approx 5 \times 10^4$ VSMCs were seeded in the top wells of Transwell-modified Boyden chambers in a 24-well Transwell dish (Corning) and allowed to attach for 30 minutes. Medium supplemented with or without PDGF-BB (20 ng/mL) was then added to the lower chamber of the Boyden chamber for 6 hours. We used 0.1% crystal violet/20% methanol to fix and stain the cells that migrated through the membranes. Five randomly chosen fields (×200) in 3 independent experiments were utilized to calculate the average number of migrated cells. The calculations were performed with the Image-Pro Plus software (version 6.0).

Quantitative Real-Time PCR and Western Blotting

We extracted total RNA from mouse carotid artery tissues with TRIzol reagent (Invitrogen). Then, cDNA

was reverse-transcribed from total RNA with the Transcriptor First Strand cDNA Synthesis Kit (Roche). SYBR Green PCR Master Mix (Applied Biosystems) was utilized to perform quantitative real-time PCR amplification according to the manufacturer's instructions. Each PCR reaction was repeated in triplicate. The primers for real-time PCR are shown in Table S2. The results of real-time PCR are presented as the average of the specific gene expression that was normalized to GAPDH gene expression.

For Western blotting, both mouse carotid artery tissues and cultured VSMCs were lysed in radioimmunoprecipitation assay lysis buffer (720 μL of radioimmunoprecipitation assay, 20 μL of phenylmethylsulfonyl fluoride, 100 μL of Complete, 100 μL of Phos-stop, 50 μL of NaF, and 10 μL of Na_3VO_4), homogenized on ice and centrifuged. Subsequently, the protein concentrations were determined using the Pierce BCA Protein Assay Kit (Pierce). Equal amounts of protein were separated by SDS-PAGE (Invitrogen) and then transferred to polyvinylidene difluoride membranes (Millipore). After blocking in 5% nonfat milk at room temperature for 60 minutes, the membranes were incubated overnight with specific primary antibodies at 4°C. The primary antibodies (Table S3) utilized in this study included rabbit anti-Tollip (ab37155; Abcam), mouse anti-PCNA (#2586; Cell Signaling Technology), rabbit anti-cyclinD1 (#2978; Cell

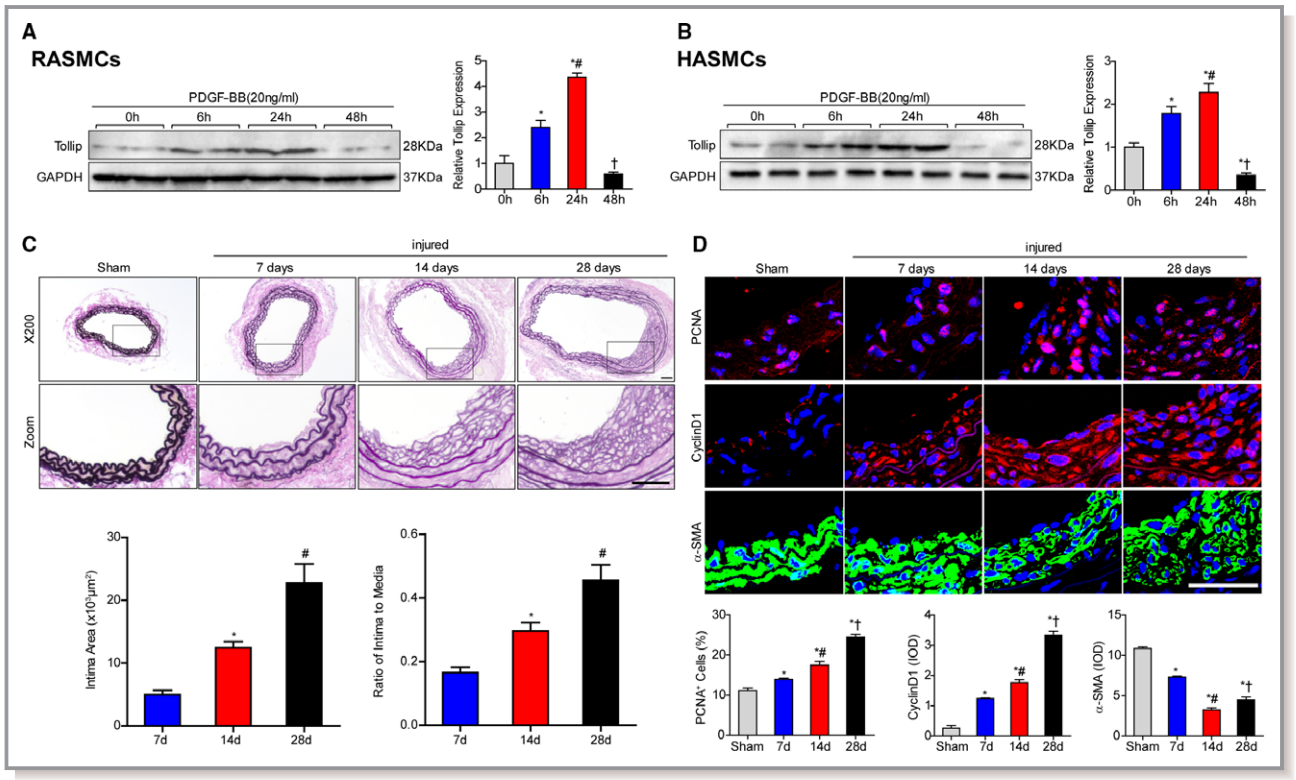

Figure 1. Vascular injury alters Tollip expression in VSMCs. A and B, Representative Western blots (left) and quantitative results (right) of Tollip protein level in RASMCs (A) or HASMCs (B) at the indicated times after PDGF-BB treatment (20 ng/mL) (n=3 independent experiments; **P*<0.05 vs 0 hour group; #*P*<0.05 vs 24 hour group; †*P*<0.05 vs 48 hour group). C, Top: Representative images of the carotid artery sections from WT mice subjected to Elastica van Gieson staining at the indicated times after wire-injury surgery. Bottom: Quantitative results of intimal area (left) and intima/media ratio (right). (n=6 each group; **P*<0.05 vs 7 days group; #*P*<0.05 vs 14 days group; scale bar, 50 μm). D, Top: Immunofluorescence staining of PCNA (red), CyclinD1 (red), and α-SMA (green) in the carotid artery sections from WT mice at the indicated times after wire-injury surgery (nucleus stained with DAPI, blue; scale bar, 50 μm). Bottom: Quantitative results of PCNA-positive cells, and expression of cyclinD1 and α-SMA in the carotid artery sections from indicated groups (n=6 each group; **P*<0.05 vs sham group; #*P*<0.05 vs 7 days group; †*P*<0.05 vs 14 days group). E, Immunofluorescence staining of Tollip (red) and α-SMA (green) in the carotid artery sections from WT mice at the indicated times after wire-injury surgery (n=6 each group; nucleus stained with DAPI, blue; scale bar, 50 μm). F, Representative Western blots (top) and quantitative results (bottom) of Tollip protein level in the carotid arteries of WT mice at the indicated times after wire-injury surgery (n=6 each group; **P*<0.05 vs sham group; #*P*<0.05 vs 14 days group). G, Immunofluorescence staining of Tollip (red) and α-SMA (green) in normal arteries (left) and restenotic arteries (right) (n=3 each group; nucleus stained with DAPI, blue; scale bar, 50 μm).GAPDH was used as a loading control in Western blot assay. DAPI indicates 4′,6-diamidino-2-phenylindole; HASMCs human aortic smooth muscle cells; PCNA, proliferating cell nuclear antigen; PDGF, platelet-derived growth factor; RASMCs, rat aortic smooth muscle cells; α-SMA, α-smooth muscle actin; VSMCs, vascular smooth muscle cells.

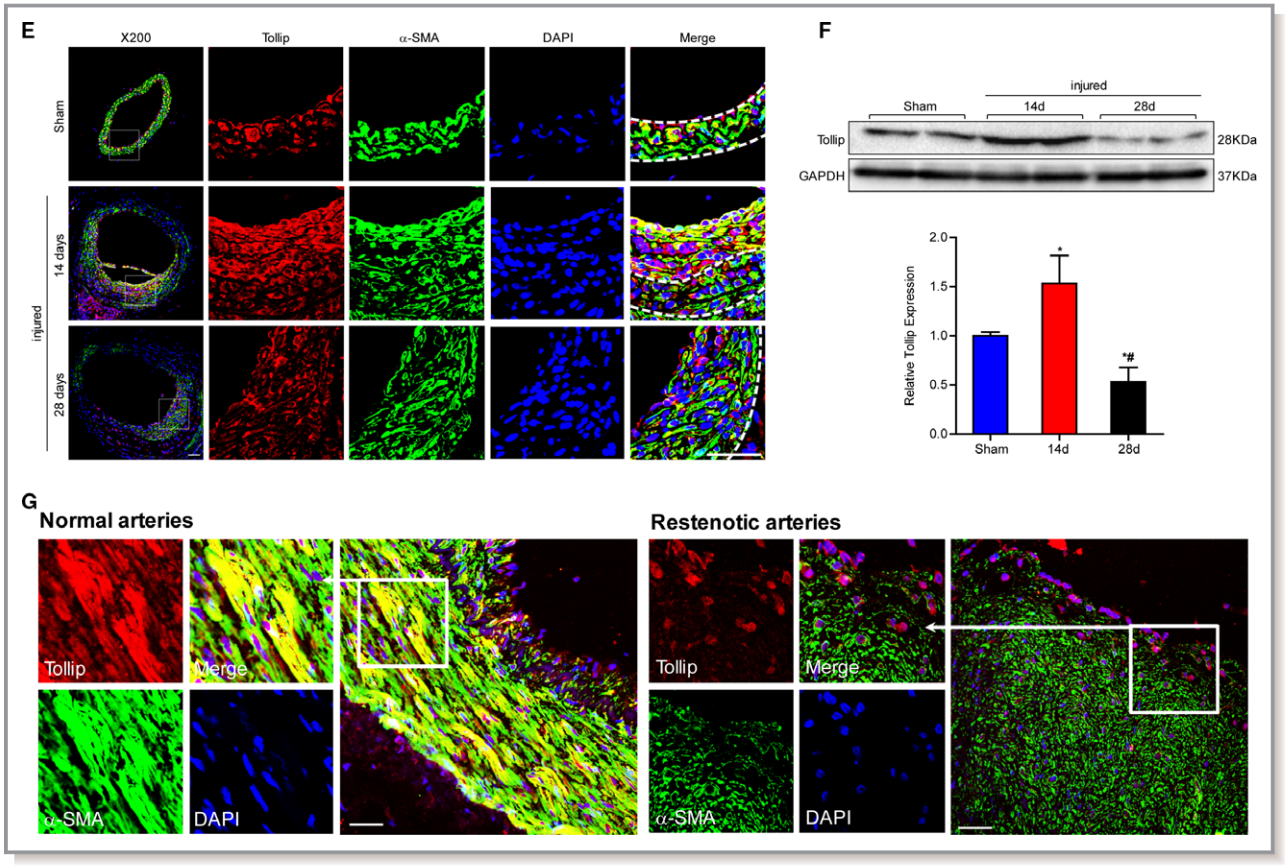

Figure 1. Continued

Signaling Technology), mouse anti-α-SMA (ab7817; Abcam), mouse anti-SM22α (ab28811; Abcam), rabbit anti-smoothelin (sc-28562; Santa Cruz), rabbit anti-MMP9 (2270; Cell Signaling Technology), rabbit anti-p-Akt (#4060; Cell Signaling Technology), rabbit anti-Akt (#4691; Cell Signaling Technology), rabbit anti-p-GSK3β (glycogen synthase kinase 3β) (sc130601; Santa Cruz), rabbit anti-GSK3β (#9315; Cell Signaling Technology), rabbit anti-p-FOXO3A (#2497; Cell Signaling Technology), rabbit anti-FOXO3A (#9465; Cell Signaling Technology), and rabbit anti-GAPDH (sc25778; Santa Cruz). After probing with the corresponding secondary antibodies at room temperature for 60 minutes, the immunoblots were visualized with the Bio-Rad ChemiDocTM XRS+. The expression levels of specific proteins were normalized to the standard housekeeping GAPDH expression levels.

Substrate Zymography

Substrate zymography was performed to measure MMP9 activity. Specifically, after electrophoresis, the samples (5 μg of protein) were subjected to gelatin (Novex 10% zymogram gel, 0.1% gelatin, Invitrogen) zymography.[14,15] Subsequently, the size-fractionated MMP proteolytic regions were measured by densitometry (Gel ProAnalyzer, Media Cybernetics).

IP Assays

Immunoprecipitation was performed as previously described.[16,17] Briefly, cultured cells were collected and lysed in immunoprecipitation buffer containing 20 mmol/L Tris-HCl (pH 8.0), 150 mmol/L NaCl, 0.5% NP-40, 1 mmol/L EDTA, and a protease inhibitor cocktail (Roche). The cell lysates were incubated with protein A agarose beads and the indicated antibodies for 3 hours at 4°C. In addition, the matrix was further washed 5 to 6 times with cold immunoprecipitation buffer and blotted using the indicated primary antibodies. Each experiment was performed in triplicate.

Statistical Analyses

The data are presented as the mean±SD. The Shapiro–Wilkinson normality test was used to test the normality of the data. For normally distributed data, the differences between 2 groups were evaluated by unpaired Student *t* tests, and the differences among multiple groups were evaluated by a 1-way ANOVA followed by the Bonferroni post hoc test (assuming

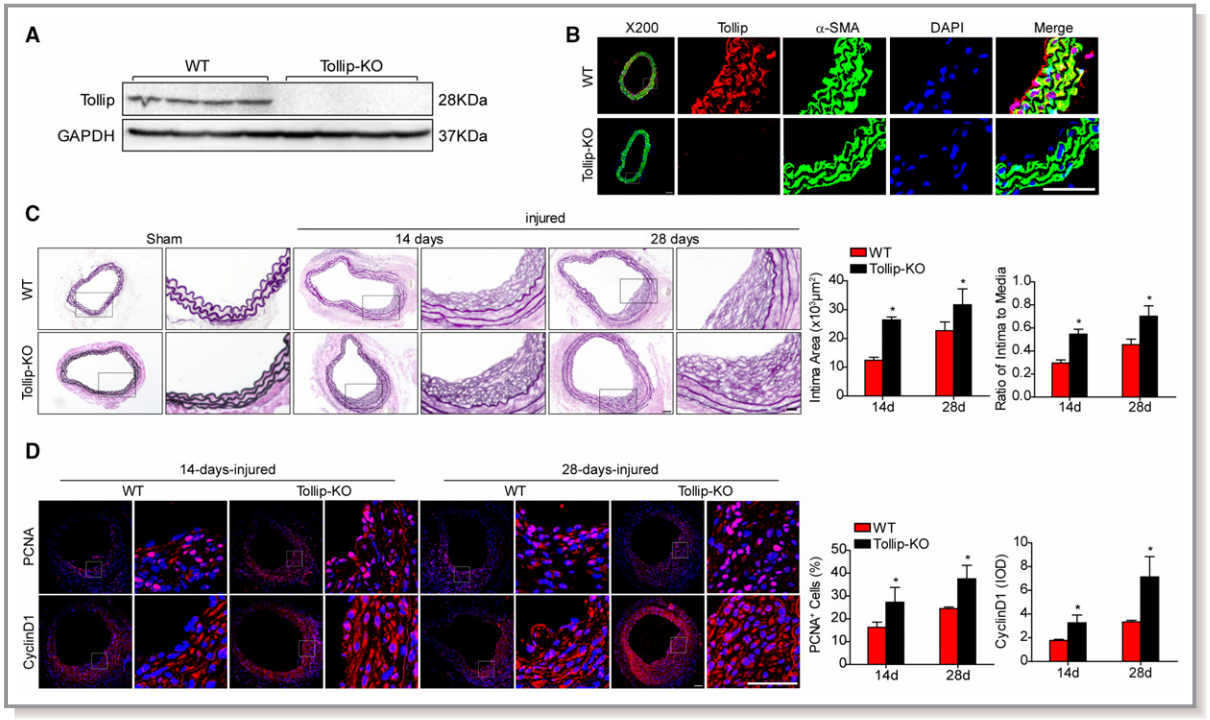

Figure 2. Tollip deficiency promotes neointima formation. A, Representative Western blots of Tollip protein level in the carotid arteries from WT and Tollip-KO mice (n=4 each group). B, Immunofluorescence staining of Tollip (red) and α-SMA (green) in the carotid arteries from WT and Tollip-KO mice at the indicated times after wire-injury surgery (n=3 each group; nucleus stained with DAPI, blue; scale bar, 50 μm). C, Left: Representative images of the left carotid artery (LCA) sections from indicated groups were subjected to Elastica van Gieson staining (scale bar, 50 μm). Right: Quantitative results of intimal area (left) and intima/media ratio (right). (n=8–10 each group, **P*<0.05 vs WT group). D, Left: Immunofluorescence staining of PCNA (red) and CyclinD1 (red) in the LCAs from indicated groups (nucleus stained with DAPI, blue; scale bar, 50 μm). Right: Quantitative results of PCNA-positive cells, and expression of CyclinD1 in the LCAs from indicated groups (n=8–10 each group, **P*<0.05 vs WT group). E, Representative Western blots (left) and quantitative results (right) of PCNA and CyclinD1 protein level in the LCAs from indicated groups. (n=6 each group; **P*<0.05 vs WT group). F, Left: Immunofluorescence staining of α-SMA (green), SM22α (green), and smoothelin (green) in the LCAs from indicated groups (nucleus stained with DAPI, blue; scale bar, 50 μm). Right: Quantitative results of α-SMA, SM22α, and smoothelin expression levels (n=8–10 each group, **P*<0.05 vs WT group). G, Representative Western blots (left) and quantitative results (right) of α-SMA, SM22α, and smoothelin protein level in the LCAs from indicated groups. (n=6 each group; **P*<0.05 vs WT group). GAPDH was used as a loading control in Western blot assay. DAPI indicates 4′,6-diamidino-2-phenylindole; KO, knockout; PCNA, proliferating cell nuclear antigen; α-SMA, α-smooth muscle actin.

equal variances) or Tamhane's T2 post hoc test (without the assumption of equal variances). For abnormally distributed data, the significant difference was determined by the Mann–Whitney *U* test or Kruskal–Wallis test. The statistical analyses were performed using SPSS software (version 17.0). A probability value (*P*) <0.05 was regarded as significant.

Results

Vascular Injury Alters Tollip Expression in VSMCs

To explore the potential function of Tollip in neointima formation, we first determined whether Tollip expression was changed in VSMCs that were challenged with PDGF-BB, a well-established stimulus of neointima formation that promotes VSMC proliferation and migration.[18] Western blot analyses were performed to examine the temporal alternation of Tollip expression in primary rat aortic smooth muscle cells and human aortic smooth muscle cells treated with PDGF-BB (20 ng/mL). Intriguingly, we observed that the protein level of Tollip in VSMCs was dramatically elevated at 6 hours after PDGF-BB treatment and peaked at 24 hours; however, the level was nearly absent at 48 hours (Figure 1A and 1B). Subsequently, we successfully established the wire-injury-induced neointima formation model, which was confirmed by the increased intimal area, I/M ratio and proliferation markers (including PCNA and cyclinD1), and the reduced expression of the differentiation marker α-smooth muscle actin (α-SMA) in the LCAs of C57BL/6 mice (Figure 1C and 1D). Immunofluorescence staining revealed that Tollip is mainly expressed in

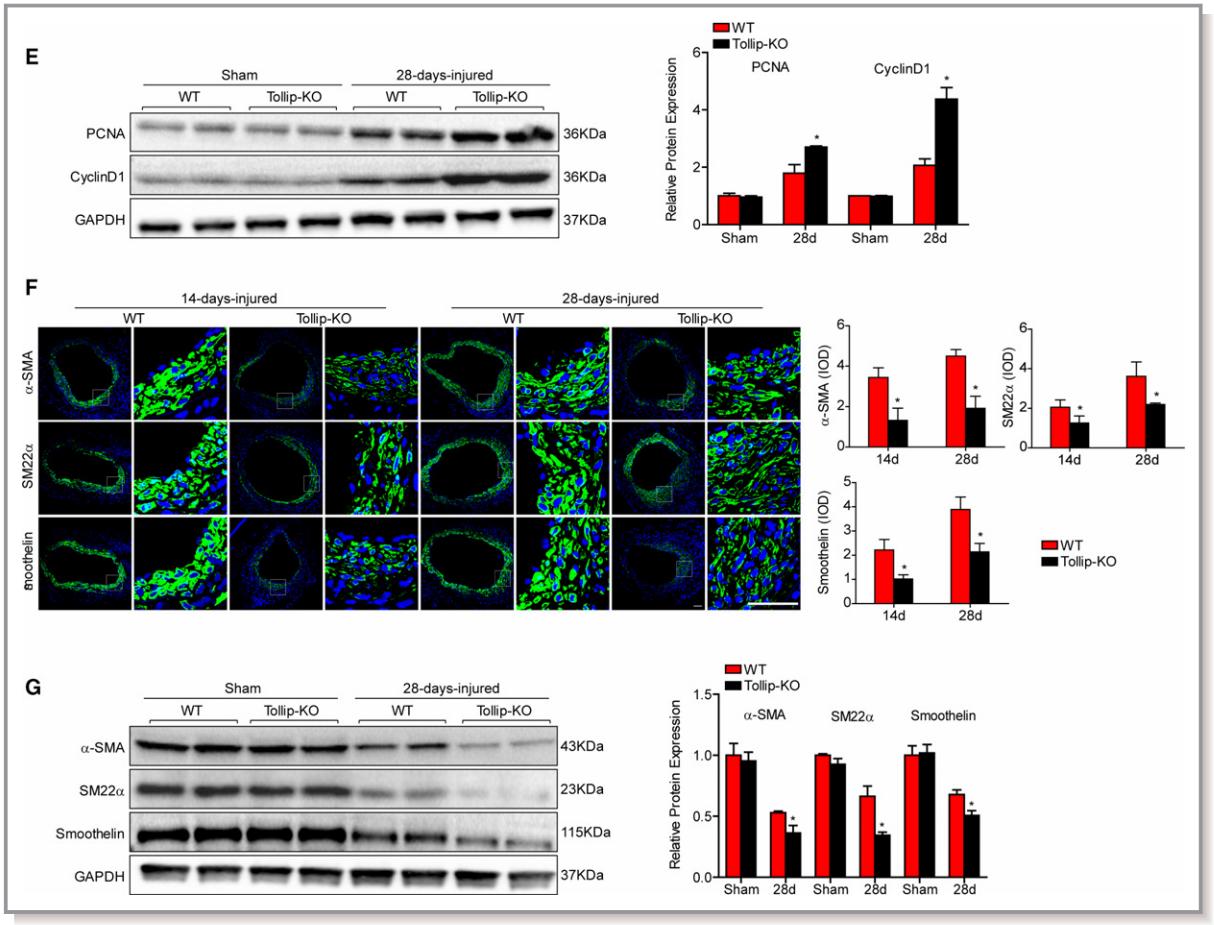

Figure 2. Continued

VSMCs (Figure 1E), as indicated by the colocalization of Tollip and α-SMA, a specific marker for VSMCs. After wire-injury surgery, the Tollip protein level was increased at 14 days but was decreased below baseline levels at 28 days (Figure 1F). In addition, we showed that the injury-induced Tollip expression occurred in the media and neointima but not in endothelial cells (Figure S1). Additional experiments showed that VSMCs in restenotic human arteries have much lower levels of Tollip than normal donor arteries (Figure 1G). Altogether, these data verified the establishment of our vascular injury model and suggest a potential involvement of Tollip in VSMC phenotypic switching and proliferation in neointima formation.

Tollip Deficiency Promotes Neointima Formation

The fluctuating Tollip expression in VSMCs upon pathological stimuli implies a regulatory effect of Tollip on neointima formation. We then generated Tollip-KO mice, which were confirmed by Western blot and immunofluorescence staining (Figure 2A and 2B). In response to the sham operation, the intimal area and I/M ratio in Tollip-KO mice were comparable to those in WT mice. However, vascular injury–induced neointima formation was strikingly exacerbated in Tollip-KO mice compared with that in their littermate controls (Figure 2C). Considering the pivotal role of VSMC proliferation in neointima formation, cellular proliferation markers, including PCNA and CyclinD1, were examined in injured LCAs from each group. Immunofluorescence staining and Western blotting analysis demonstrated that Tollip-KO mice expressed much higher levels of PCNA and CyclinD1 in injured LCAs than WT mice (Figure 2D and 2E). Consistently, compared with WT controls, the dedifferentiation of VSMCs after vascular injury was further enhanced by the Tollip deficiency, as evidenced by the diminished expression of VSMC differentiation markers (α-SMA, SM22, and smoothelin) (Figure 2F and 2G). Therefore, our results indicate that ablation of Tollip may contribute to intimal hyperplasia by promoting VSMC phenotypic switching and proliferation.

SMC-Specific Tollip Overexpression Attenuates Neointima Formation

Based on the data from loss-of-function experiments, we hypothesized that Tollip overexpression in VSMCs possesses therapeutic potential to inhibit intimal hyperplasia. To confirm

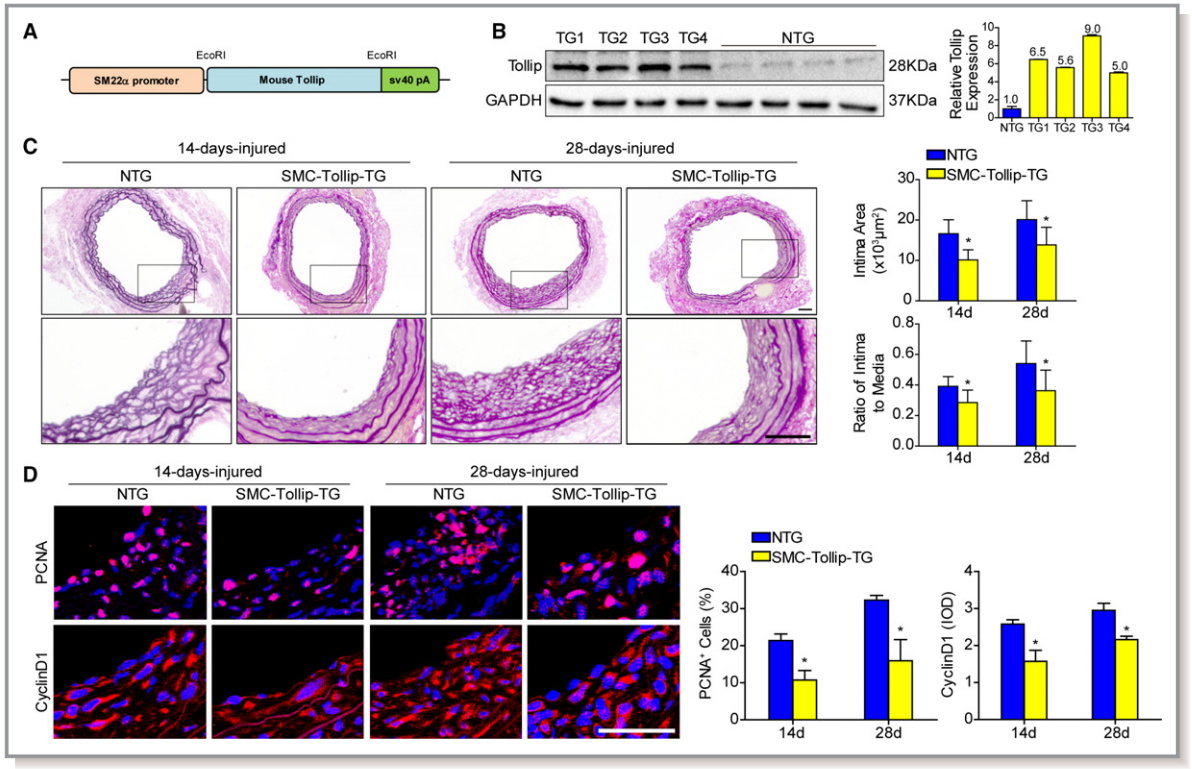

Figure 3. SMC-specific Tollip overexpression attenuates neointima formation. A, Schematic diagram of the construction of transgenic (TG) mice harboring a full-length mouse Tollip cDNA under the control of the SM22α promoter. B, Representative Western blots (left) and quantitative results (right) of Tollip expression levels in the carotid arteries of 4 TG lines and their NTG controls (n=3 independent experiments). C, Left: representative images of the left carotid artery sections from NTG or Tollip-TG mice at indicated times after wire-injury surgery subjected to EVG staining (scale bar, 50 μm). Right: quantitative results of intimal area and intima/media ratio. (n=8–10 each group, **P*<0.05 vs NTG group). D, Left: immunofluorescence staining of PCNA (red) and CyclinD1 (red) in the LCAs from indicated groups (nucleus stained with DAPI, blue; scale bar, 50 μm). Right: quantitative results of PCNA-positive cells, and expression of cyclinD1 (n=8–10 each group, **P*<0.05 vs NTG group). E, Representative Western blots (left) and quantitative results (right) of PCNA and CyclinD1 protein level in the LCAs from indicated groups. (n=6 each group; **P*<0.05 vs NTG group). F, Left: immunofluorescence staining of α-SMA (green), SM22α (green), and smoothelin (green) in the LCAs from indicated groups (nucleus stained with DAPI, blue; scale bar, 50 μm). Right: quantitative results of α-SMA, SM22α, and smoothelin expression levels (n=8–10 each group, **P*<0.05 vs NTG group). G, Representative Western blots (left) and quantitative results (right) of α-SMA, SM22α, and smoothelin protein level in the LCAs from indicated groups. (n=6 each group; **P*<0.05 vs NTG group). GAPDH was used as a loading control in Western blot assay. DAPI indicates 4′,6-diamidino-2-phenylindole; EVG, Elastica van Gieson; NTG, nontransgenic; PCNA, proliferating cell nuclear antigen; α-SMA, α-smooth muscle actin; SMC, smooth muscle cell; TG, transgenic.

this hypothesis, 4 independent lines of SMC-specific Tollip-overexpressing mice (TG1, TG2, TG3, and TG4) were generated (Figure 3A), which have been tested by Western blot (Figure 3B) and immunofluorescence staining (Figure S2). The TG3 line had the highest protein expression of Tollip and was selected for use in the following experiments. Upon sham operation, the extent of intimal hyperplasia in the LCAs was comparable between Tollip-TG mice and their NTG littermates (data not shown). However, the intimal area and I/M ratio in Tollip-TG mice were much lower than those in NTG mice after carotid artery wire injury (Figure 3C). In response to vascular injury, Tollip-overexpressing mice exhibited blunted cellular proliferation in the LCA compared with that in the NTG mice, as evidenced by the decreased expression of PCNA and cyclinD1 (Figure 3D and 3E). In addition, both immunofluorescence staining and Western blotting analysis demonstrated that the ameliorated proliferation in Tollip-TG arteries was concomitant with an elevation in the expression levels of differentiation markers, including α-SMA, SM22a, and smoothelin, compared with the expression levels in their littermate controls (Figure 3F and 3G). Taken together, our data support the hypothesis that VSMC-derived Tollip is critical for the prevention of VSMC phenotypic switching and proliferation and the subsequent neointima formation.

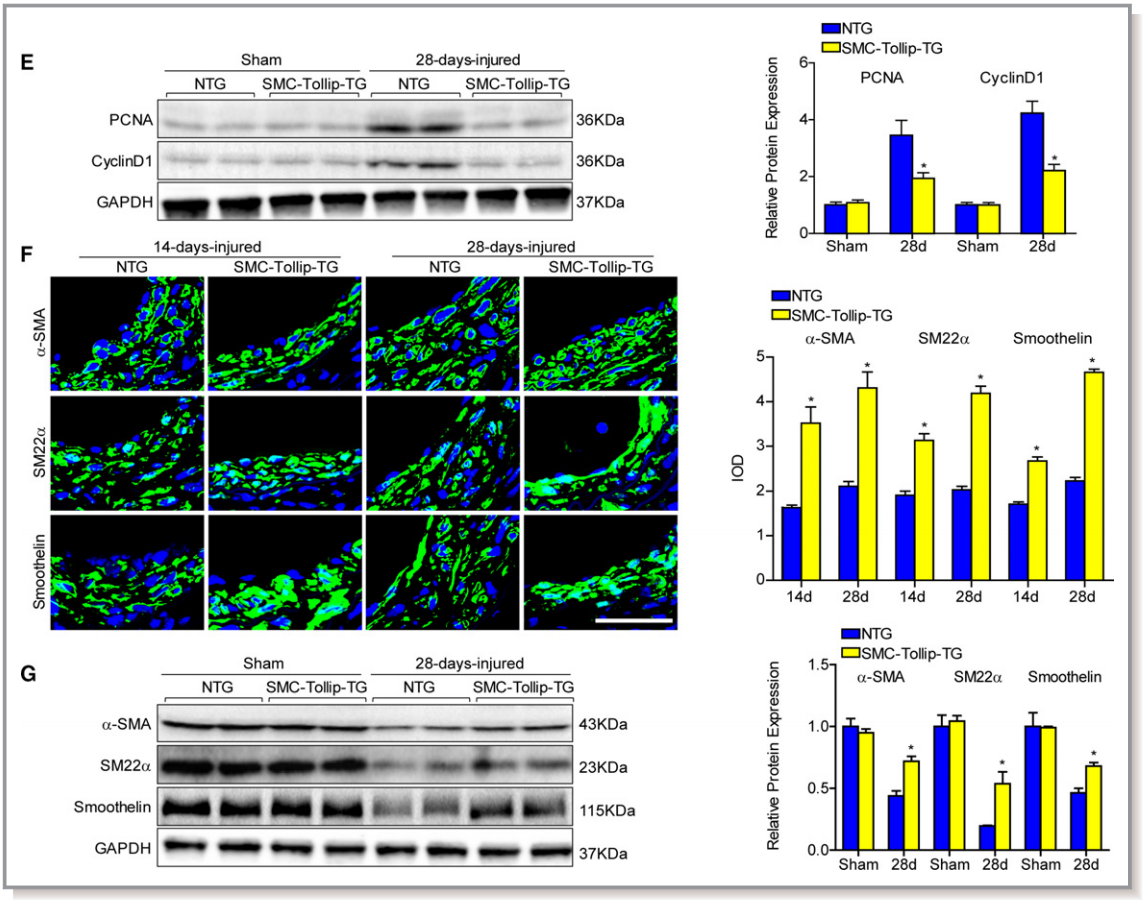

Figure 3. Continued

Tollip Inhibits PDGF-BB-Induced VSMC Proliferation, Phenotypic Switching, and Migration

Given that the impact of Tollip on neointimal formation may conducted by cellular components of artery other than VSMCs, VSMCs separated from Tollip-KO mice, Tollip-TG mice, and their littermate controls were utilized in our in vitro experiments. In response to PDGF-BB (20 ng/mL) treatment, the proliferation markers were progressively upregulated, whereas the differentiation markers sharply downregulated in the control groups. Notably, the PDGF-BB-induced VSMC proliferation and phenotype switching were further augmented by Tollip deficiency (Figure 4A). Accordingly, Tollip-overexpressing VSMCs expressed lower levels of proliferation markers, but higher levels of differentiation markers compared with the controls after PDGF-BB administration (Figure 4B). Moreover, we observed that the regulatory effect of Tollip on VSMC proliferation and differentiation was independent of its secretion, since addition of Tollip antibody did not affect the effect of PDGF-BB on VSMC (Figure S3). In addition to proliferation and phenotypic switching, the migrating VSMCs participate in the pathogenesis of neointima formation.[19] To elucidate the role of Tollip in the migratory property of VSMCs, primary VSMCs derived from Tollip-KO and Tollip-TG mice were seeded into a Boyden chamber supplemented with or without PDGF-BB (20 ng/mL) for 6 hours. The extent of VSMC migration in the control groups (WT and NTG groups) was strongly induced by PDGF-BB administration and was further exacerbated by Tollip ablation; however, this migration was significantly suppressed by Tollip overexpression (Figure 4C). Given the involvement of MMPs, especially MMP9, in VSMC migration and the subsequent neointima formation,[20,21] real-time PCR assays were performed to determine the mRNA levels of MMP9 in Tollip-KO and Tollip-TG LCAs subjected to sham or wire injury surgery. Upon sham operation, the MMP9 expression level was not altered among the groups. However, the wire-injury-induced increase in MMP9 expression was significantly aggravated by Tollip deficiency but attenuated by Tollip overexpression (Figure 4D through 4F). These results were further confirmed by the substrate zymography assays (Figure 4G and 4H). Therefore, in addition to the regulatory effect on VSMC phenotypic switching and proliferation, Tollip also prevents intimal hyperplasia by inhibiting VSMC migration.

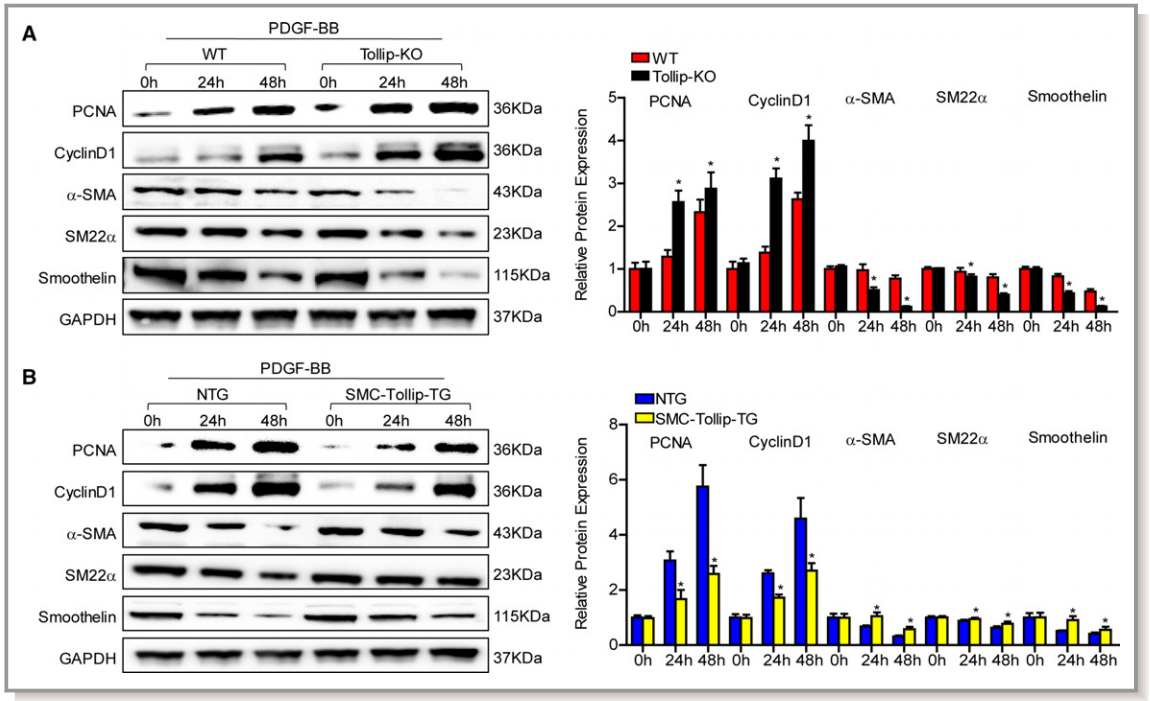

Figure 4. Tollip inhibits PDGF-BB-induced VSMC proliferation, phenotypic switching, and migration. A and B, Representative Western blots (left) and quantitative results (right) of PCNA, CyclinD1 α-SMA, SM22α, and smoothelin protein level in the VSMCs from indicated groups. (n=4 each group; **P*<0.05 vs WT or NTG group). C, Top: Representative images of the transwell assays that were performed to determine the VSMCs migration in indicated groups (scale bar, 50 μm). Bottom: the number of migrated VSMCs were counted in 5 high-power fields (×200) from each group (n=3 independent experiments; **P*<0.05 vs WT or NTG group). D and E, Real-time PCR assays were performed to determine the relative mRNA levels of MMP9 in the LCAs from indicated groups (n=4 each group; **P*<0.05 vs WT or NTG group). F, The MMP9 expression tested by immunofluorescence staining (n=4 each group; **P*<0.05 vs WT or NTG group). G and H, The substrate zymography assays were performed to determine the activity of MMP-9 in the LCAs from indicated groups (n=4 each group; **P*<0.05 vs WT or NTG group). LCAs indicates left carotid arteries; NTG, nontransgenic; PCNA, proliferating cell nuclear antigen; PCR, polymerase chain reaction; PDGF, platelet-derived growth factor; α-SMA, α-smooth muscle actin; VSMC, vascular smooth muscle cells.

AKT-Dependent Signaling Is Required for the Regulatory Effects of Tollip on Neointima Formation

Although we demonstrated the regulatory effect of Tollip on neointima formation, the underlying mechanism remains to be determined. Because Akt plays a critical role in the pathophysiology of VSMC remodeling and the capacity of Tollip to modulate adverse cardiac remodeling through Akt-dependent pathways have been established,[8–10,22,23] we hypothesized that Akt might also be required for the regulatory effects of Tollip on neointima formation. Western blotting was then performed to delineate the expression and phosphorylation of Akt and its downstream molecules, including GSK3β and FOXO3A, in LCAs from each group. Neither the alternation of Tollip expression nor vascular injury affected the total expression of Akt-dependent molecules. However, compared with the control groups, the wire-injury-induced phosphorylation of Akt-dependent molecules was enhanced by Tollip deficiency but significantly suppressed by Tollip overexpression (Figure 5A). Moreover, the co-immunoprecipitation experiments were performed in VSMCs treated with PBS or PDGF-BB to identify whether Tollip directly regulate Akt. Our data showed that Tollip could interact with Akt weakly at baseline (PBS), but this interaction was significantly enhanced by PDGF-BB administration (Figure 5B).

These results suggest that Tollip exerts a protective function on intimal hyperplasia by inhibiting the activation of Akt-dependent signaling.

To confirm our hypothesis that Tollip may suppress intimal hyperplasia in an Akt-dependent manner, an AKTI was intraperitoneally injected every 3 days from 1 week before surgery to 4 weeks after the wire-injury operation, and the extent of neointima formation was determined at 4 weeks postinjury. The inhibitory effect of AKTI on Akt-dependent signaling molecules was confirmed by Western blot and immunofluorescence staining analyses (Figure 5C and Figure S4). As predicted, AKTI reversed the worsened intimal

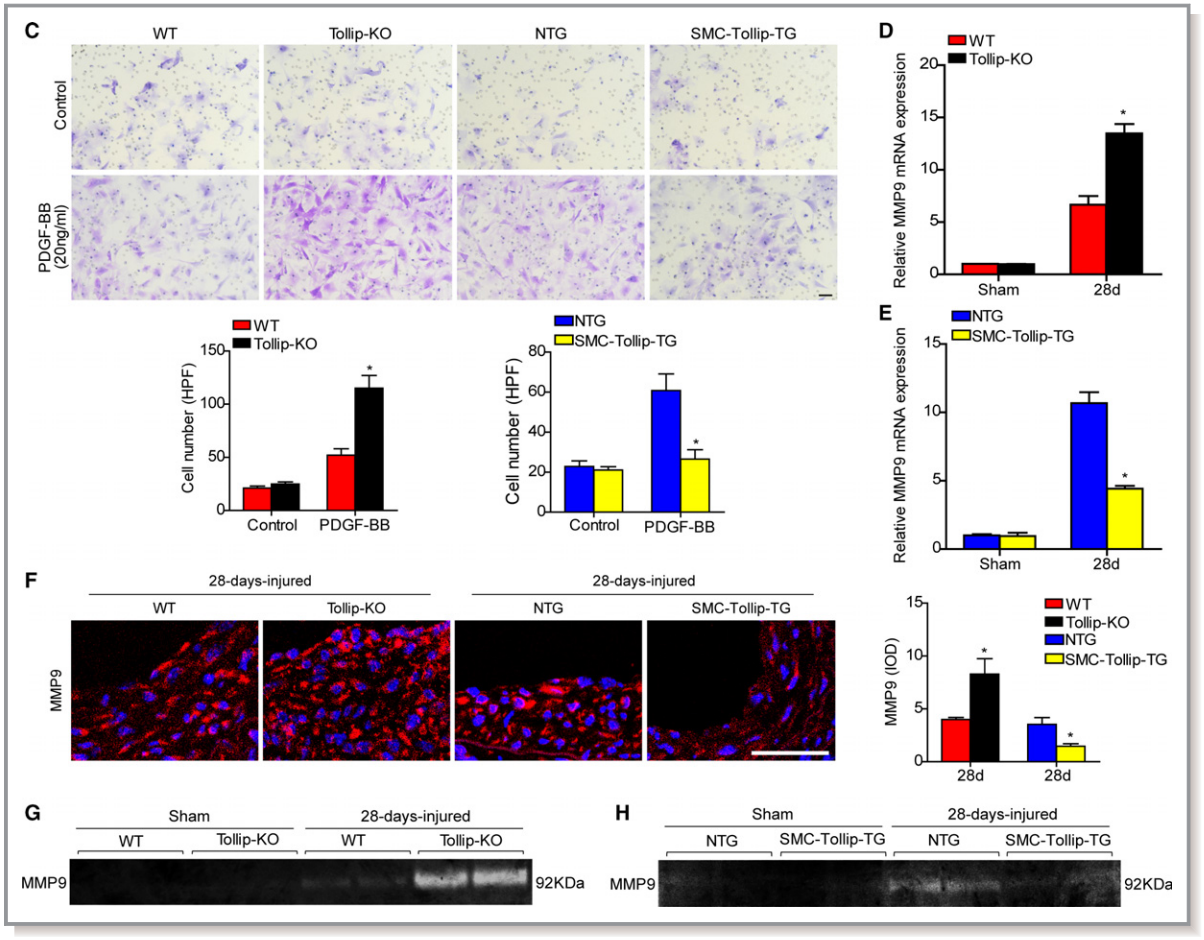

Figure 4. Continued

hyperplasia in Tollip-KO mice. This conclusion was drawn from the following observations made in wire-injury-induced Tollip-KO mice that were administered AKTI compared with Tollip-KO mice treated with PBS: (1) decreased intimal area and I/M ratio (Figure 5D), (2) reduced expression of PCNA and cyclinD1 (Figure 5E), and (3) preserved expression of α-SMA (Figure 5E).

Tollip Deletion Accelerates Neointima Formation in Rats

Because pathological neointima formation may vary significantly among different animal models, we further tested the beneficial effects of Tollip in the well-established carotid balloon injury rat model. The Tollip-KO rat was generated as previously described.[24] In agreement with the data from mice, the indexes of pathological neointima formation were largely exaggerated in Tollip-KO rats compared with those in the WT controls, as evidenced by increased intimal area, I/M ratio and proliferation indexes, and decreased expression of differentiation markers (Figure 6A through 6C). Therefore, the detrimental effect of Tollip deletion in the carotid balloon injury rat model provides additional evidence for the critical function of Tollip in intimal hyperplasia.

Discussion

Neointima formation, which mainly results from VSMC dedifferentiation, migration, and proliferation, is the major factor that reduces revascularization therapy efficiency. In the present study, through both loss-of- and gain-of-function approaches, we provide the first evidence that Tollip exerts a protective effect on this pathophysiological process by suppressing VSMC dedifferentiation, migration, and proliferation.

In addition to the well-established role of TLR signaling in the immune system, increasing evidence suggests that TLR signaling exerts a crucial effect on the pathogenesis of multiple cardiovascular diseases.[25,26] In the vasculature, activated TLR signaling increases VSMC phenotypic switching, proliferation, and migration, which are essential processes in neointima formation.[12,13,27] This evidence suggests that targeting TLR signaling may be a novel therapeutic target for treating neointima formation. Tollip is a widely accepted regulator of TLR signaling in the immune response, suggesting

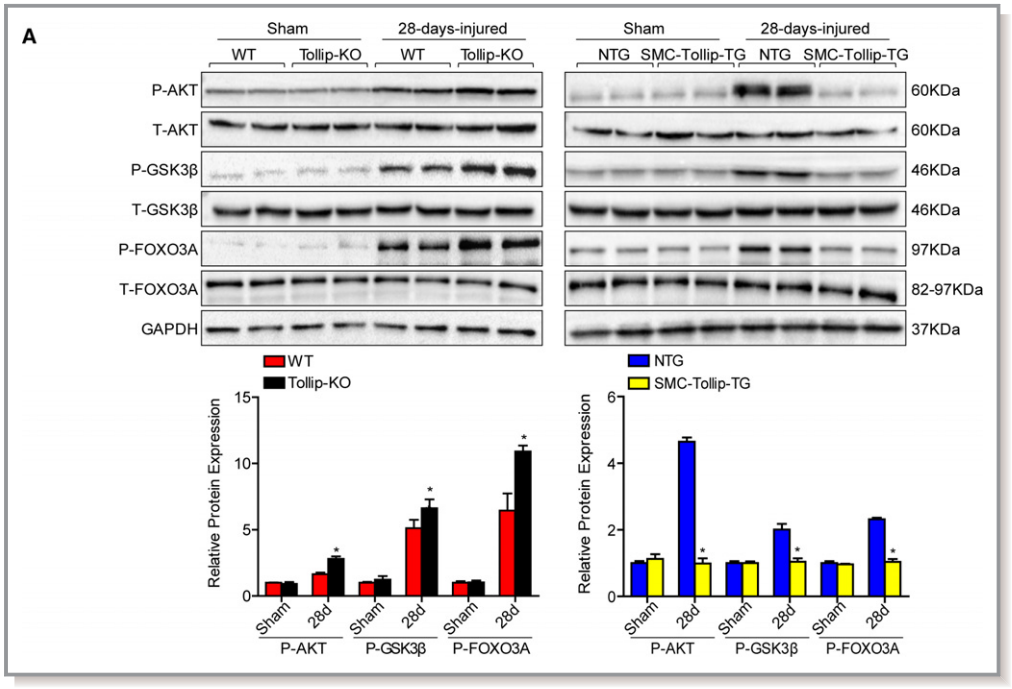

Figure 5. AKT-dependent signaling is required for the regulatory effects of Tollip on neointima formation. A, Representative Western blots (top) and quantitative results (bottom) of total and phosphorylated levels of Akt-dependent signaling molecules in the LCAs from indicated mice after 28 days of sham or wire-injury surgery (n=4 each group; **P*<0.05 vs WT or NTG group). B, Western blots were performed with Tollip or AKT antibody after co-IP of Tollip from VSMCs lysates subjected to PBS or PDGF-BB administration. C, Representative Western blots (left) and quantitative results (right) of total and phosphorylated levels of Akt and GS3K-β in the LCAs from PBS- or AKTI-treated Tollip-KO mice after 28 days of wire-injury surgery (n=4 each group; **P*<0.05 vs PBS group). D, Left: Representative images of the LCA sections from indicated groups subjected to EVG staining (scale bar, 50 μm). Right: Quantitative results of intimal area and intima/media ratio. (n=6–8 each group; **P*<0.05 vs WT/PBS; #*P*<0.05 vs WT/AKTI; †*P*<0.05 vs Tollip-KO/PBS). E, Left: Immunofluorescence staining of PCNA (red), CyclinD1 (red), and α-SMA (green) in the LCAs of indicated groups (nucleus stained with DAPI, blue; scale bar, 50 μm). Right: Quantitative results of PCNA-positive cells, and expression of cyclinD1 and α-SMA (n=6–8 each group; **P*<0.05 vs WT/PBS; #*P*<0.05 vs WT/AKTI; †*P*<0.05 vs Tollip-KO/PBS). GAPDH was used as a loading control in Western blot assay. ATKI indicates AKT inhibitor; EVG, Elastica van Gieson; IP, immunoprecipitation; LCA, left carotid artery; NTG, nontransgenic; P, phosphorylated; PBS, phosphate-buffered saline; PDGF, platelet-derived growth factor; PCNA, proliferating cell nuclear antigen; VSMC, vascular smooth muscle cells.

that Tollip may play a role in the development of neointima formation. Because its regulatory function can be predicted by altering its expression under certain pathophysiological conditions, we examined whether Tollip expression levels are varied during neointima hyperplasia. In the present study, a transient increase in Tollip expression was observed in VSMCs after vascular injury. The early induction of Tollip in VSMCs may exert a compensatory action against such acute stimuli. However, this moderate increase in Tollip expression was insufficient to neutralize the detrimental effects of vascular injury. By contrast, the expression level of Tollip was nearly depleted by the late phase of vascular repair. This phenomenon is consistent with previous findings that Tollip levels are significantly elevated by acute stimuli, such as myocardial infarction, but are attenuated in a chronic pressure overload model.[9,10] However, the precise regulatory mechanism of Tollip expression was not clarified in the present study; therefore, additional experiments are still required to decipher it.

Under basal conditions, highly differentiated VSMCs reside in the media of vessels and exhibit contractile properties with insignificant proliferative and migratory capacity.[28] However, these VSMCs retain the ability to adjust their phenotype based on the changing local environment. Specifically, in response to inevitable vascular injury during revascularization treatment, VSMCs dedifferentiate from a contractile to a synthetic phenotype that is characterized by increased migration and proliferation activity and decreased levels of smooth muscle–specific contractile proteins.[29] Although the migration and proliferation of dedifferentiated VSMCs in the

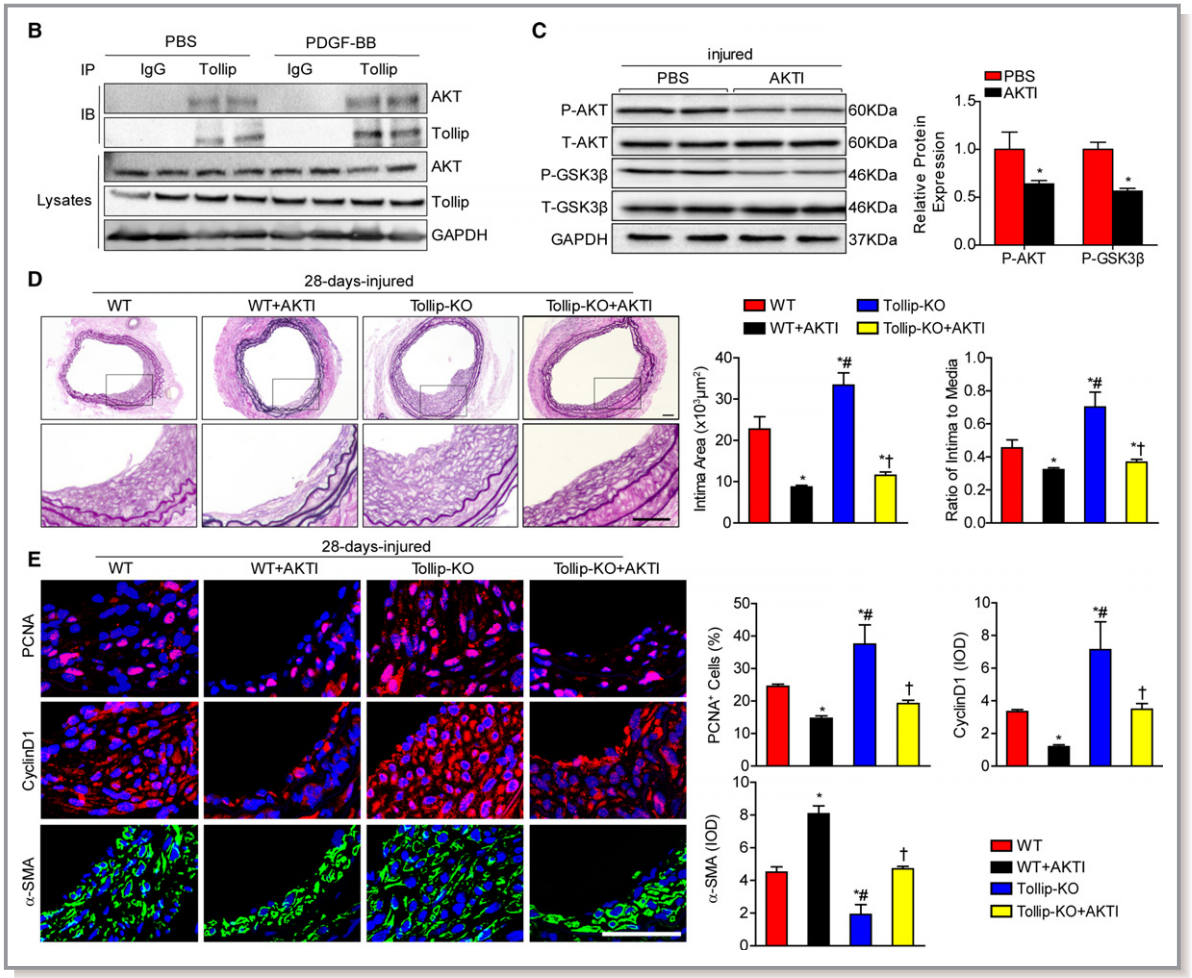

Figure 5. Continued

vascular wall initially represents a critical mechanism for vascular healing, this process would eventually progress into intimal hyperplasia and luminal stenosis.[30] To investigate the role of Tollip in VSMC phenotypic switching, migration, proliferation, and the subsequent neointima formation, we used loss- and gain-of-function approaches in both in vivo and in vitro experiments. The protective role for Tollip was supported by the finding that systemic Tollip-KO mice displayed aggravated intimal hyperplasia after vascular injury. Because the systemic deletion of Tollip may influence vascular cells other than VSMCs, VSMC-specific Tollip-overexpressing mice and genetically modified primary VSMCs were used to affirm whether Tollip mainly exerts its protective effects in a VSMC-dependent or VSMC-independent manner. Although we cannot exclude the possibility that Tollip affects vascular cells other than VSMCs during vascular injury–mediated neointima formation, we can conclude that Tollip suppresses these pathological conditions, at least partially, by regulating VSMC phenotypic switching, migration, and proliferation. These findings are consistent with previous research that Tollip deletion renders a stable atherosclerosis phenotype with increased smooth muscle cells.[31] Meanwhile, Chen et al observed the reduced systemic inflammation in ApoE$^{-/-}$/Tollip$^{-/-}$ mice. Therefore, they presumed that the reduced systemic inflammation caused by Tollip deletion may be the underlying mechanism for the increased SMCs. According to our results, although we could not exclude the possibility that VSMC-derived Tollip may inhibit VSMC proliferation by regulating the systemic or regional inflammation, the antiproliferation effect of Tollip can also be explained by its negative action on the activation of Akt signaling and the expression of proliferation-associated molecules (PCNA and CyclinD) in VSMCs. However, additional experiments are still required to confirm our hypothesis.

It is important to elucidate the molecular mechanism by which Tollip regulates VSMC function and subsequent neointima formation. As a well-established signaling cascade that participates in intimal hyperplasia, Akt signaling is also a downstream pathway of Tollip in cardiovascular disease.[8–10,22,23] Therefore, we investigated the status of the Akt-dependent signaling pathway in response to vascular injury. Consistent with previous studies, we observed a

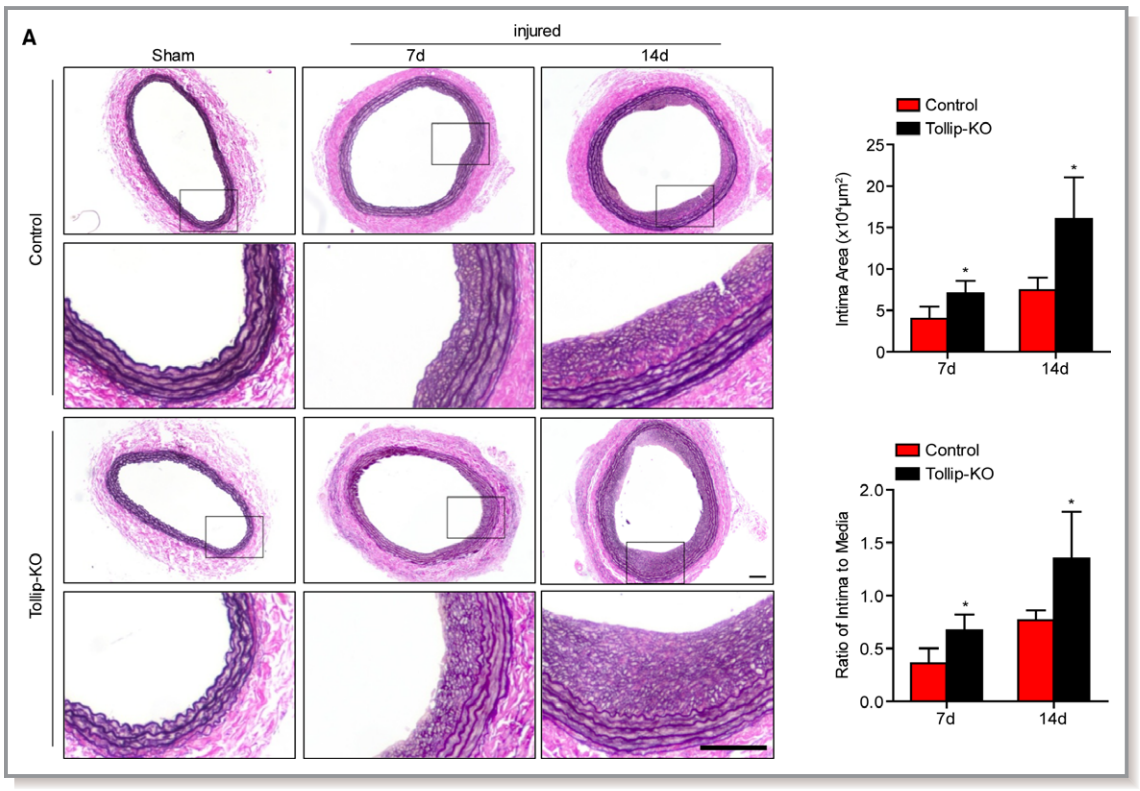

Figure 6. Tollip deletion accelerates neointima formation in rats. A, Left: Representative images of the LCA sections from indicated groups subjected to EVG staining (scale bar, 100 μm). Right: Quantitative results of intimal area and intima/media ratio. (n=6 each group; **P*<0.05 vs control group). B, Left: Immunofluorescence staining of PCNA (red) and α-SMA (green) in the LCAs of indicated groups (nucleus stained with DAPI, blue; scale bar, 100 μm). Right: Quantitative results of PCNA-positive cells and expression of α-SMA (n=6 each group; **P*<0.05 vs control group). C, Representative Western blots (left) and quantitative results (right) of PCNA, CyclinD1, and α-SMA protein level in the LCAs from indicated groups. (n=4 each group; **P*<0.05 vs control group). GAPDH was used as a loading control in Western blot assay. DAPI indicates 4′,6-diamidino-2-phenylindole; LCA, left carotid artery; PCNA, proliferating cell nuclear antigen; α-SMA, α-smooth muscle actin.

negative relationship between the Tollip expression level and the Akt signaling activation. Additionally, the exaggerated VSMC phenotypic switching, proliferation, and neointima formation in Tollip-KO mice were reversed by a pharmacological Akt-specific inhibitor. These data suggest that Tollip negatively regulates the pathogenesis of neointima formation, mainly through the inactivation of Akt-dependent signaling. In addition, the directly regulatory action of Tollip on Akt was further confirmed by Co-IP experiments. However, the role of Akt signaling in VSMCs and neointima formation remains controversial. In contrast to its previously reported detrimental role, some studies also found that Akt signaling, especially when induced by insulin-like growth factor, maintains the differentiated VSMC phenotype and inhibits VSMC migration and proliferation.[32,33] One possible explanation for this contradiction could be because of the distinct physiological functions of different Akt isoforms in VSMCs. Among the 3 Akt isoforms, Akt1 and Akt2 are ubiquitously expressed, including in VSMCs, but Akt3 is primarily expressed in the brain.[34] Genetic manipulation of Akt1 or Akt2 in mice or VSMCs has revealed that Akt1 contributes to VSMC proliferation and migration, whereas Akt2 is necessary for the inhibition of VSMC phenotypic switching, migration, and proliferation.[30,35–37] Alternatively, numerous studies have shown that Akt activation triggered by vascular injury and PDGF-BB treatment leads to VSMC migration and proliferation, whereas other studies have elucidated the opposite effect following insulin-like growth factor–induced Akt activation.[22,23,30] Therefore, the role of Akt in neointima formation may also depend on the isoform and upstream stressors. Nevertheless, our study did not clearly validate the molecular mechanisms through which Tollip modulates Akt-dependent signaling or the exact Akt isoform that mediates the protective action of Tollip in VSMCs. Thus, further investigations on these issues are still needed.

Up to now, genetically engineered mice have been widely used as mammalian models for biomedical research. However, the physiological differences between humans and mice limit

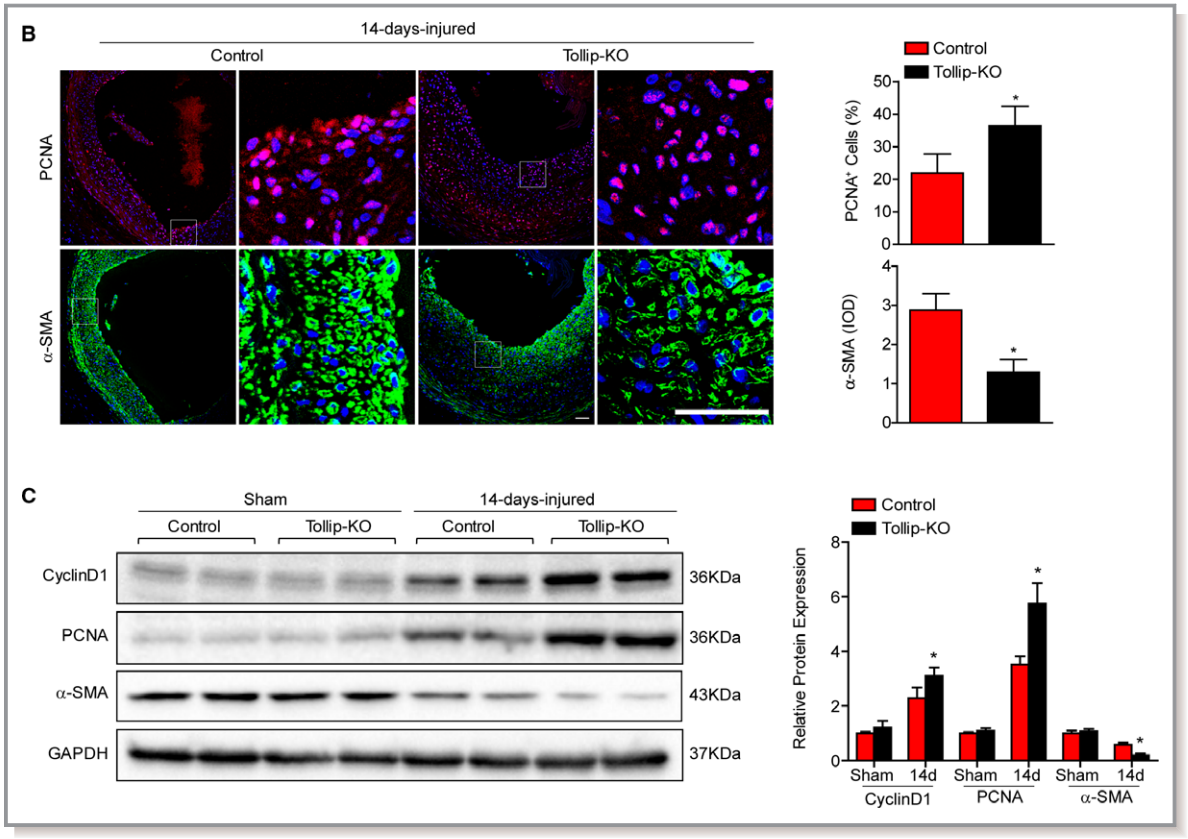

Figure 6. Continued

the clinical application of the experimental findings.[38] Because the rat more closely resembles humans physiologically, along with recent advances in CRISPR-Cas9 technology, we successfully generated genetically modified rats with which to test the regulatory role of Tollip in neointima formation. Consistent with the results from the mouse experiments, the exaggerated intimal hyperplasia in Tollip-KO rats subjected to carotid injury confirms the role of Tollip in neointima formation and highlights its therapeutic potential.

In this study, we provide the first evidence that Tollip is a novel, bona fide suppressor of neointima formation that exerts its effects through the inhibition of VSMC phenotypic switching, migration, and proliferation. The protective action of Tollip on neointima formation seems to rely on the inhibition of Akt signaling. Therefore, our findings not only broaden our knowledge of the molecular mechanisms underlying neointima formation but also suggest the therapeutic potential of Tollip in the treatment of neointima formation and luminal stenosis after revascularization therapy.

Sources of Funding

This work was supported by grants from the National Science Fund for Distinguished Young Scholars (No. 81425005), the Key Project of the National Natural Science Foundation (No. 81330005), the National Natural Science Foundation of China (Nos. 81470474, 81370209, 81370365, 81270184, 31371481, and 91639304), and the National Science and Technology Support Project (Nos. 2013YQ030923-05, 2014BAI02B01, 2015BAI08B01, and 2016YFF0101500).

Disclosures

None.

References

1. Stone NJ, Robinson JG, Lichtenstein AH, Bairey Merz CN, Blum CB, Eckel RH, Goldberg AC, Gordon D, Levy D, Lloyd-Jones DM, McBride P, Schwartz JS, Shero ST, Smith SC Jr, Watson K, Wilson PW, Eddleman KM, Jarrett NM, LaBresh K, Nevo L, Wnek J, Anderson JL, Halperin JL, Albert NM, Bozkurt B, Brindis RG, Curtis LH, DeMets D, Hochman JS, Kovacs RJ, Ohman EM, Pressler SJ, Sellke FW, Shen WK, Smith SC Jr, Tomaselli GF; American College of Cardiology/American Heart Association Task Force on Practice G. 2013 ACC/AHA guideline on the treatment of blood cholesterol to reduce atherosclerotic cardiovascular risk in adults: a report of the American College of Cardiology/American Heart Association Task Force on Practice Guidelines. *Circulation*. 2014;129:S1–S45.
2. Dzau VJ, Braun-Dullaeus RC, Sedding DG. Vascular proliferation and atherosclerosis: new perspectives and therapeutic strategies. *Nat Med*. 2002;8:1249–1256.
3. Er OB, Ma X, Simard T, Pourdjabbar A, Hibbert B. Pathogenesis of neointima formation following vascular injury. *Cardiovasc & Hematol Disord Drug Targets*. 2011;11:30–39.

4. Weintraub WS. The pathophysiology and burden of restenosis. *Am J Cardiol*. 2007;100:3K–9K.
5. Kawai-Kowase K, Owens GK. Multiple repressor pathways contribute to phenotypic switching of vascular smooth muscle cells. *Am J Physiol Cell Physiol*. 2007;292:C59–C69.
6. Hao H, Gabbiani G, Bochaton-Piallat ML. Arterial smooth muscle cell heterogeneity: implications for atherosclerosis and restenosis development. *Arterioscler Thromb Vasc Biol*. 2003;23:1510–1520.
7. Capelluto DG. Tollip: a multitasking protein in innate immunity and protein trafficking. *Microbes Infect*. 2012;14:140–147.
8. Hu Y, Li T, Wang Y, Li J, Guo L, Wu M, Shan X, Que L, Ha T, Chen Q, Kelley J, Li Y. Tollip attenuated the hypertrophic response of cardiomyocytes induced by IL-1beta. *Front Biosci*. 2009;14:2747–2756.
9. Liu Y, Jiang XL, Liu Y, Jiang DS, Zhang Y, Zhang R, Chen Y, Yang Q, Zhang XD, Fan GC, Li H. Toll-interacting protein (Tollip) negatively regulates pressure overload-induced ventricular hypertrophy in mice. *Cardiovasc Res*. 2014;101:87–96.
10. Wan N, Liu X, Zhang XJ, Zhao Y, Hu G, Wan F, Zhang R, Zhu X, Xia H, Li H. Toll-interacting protein contributes to mortality following myocardial infarction through promoting inflammation and apoptosis. *Br J Pharmacol*. 2015;172:3383–3396.
11. Zhang G, Ghosh S. Negative regulation of Toll-like receptor-mediated signaling by Tollip. *J Biol Chem*. 2002;277:7059–7065.
12. Wang B, Zhang L, Zhang T, Wang H, Zhang J, Wei J, Shen B, Liu X, Xu Z, Zhang L. *Chlamydia pneumoniae* infection promotes vascular smooth muscle cell migration through a Toll-like receptor 2-related signaling pathway. *Infect Immun*. 2013;81:4583–4591.
13. de Graaf R, Kloppenburg G, Kitslaar PJ, Bruggeman CA, Stassen F. Human heat shock protein 60 stimulates vascular smooth muscle cell proliferation through Toll-like receptors 2 and 4. *Microbes Infect*. 2006;8:1859–1865.
14. Spinale FG, Escobar GP, Hendrick JW, Clark LL, Camens SS, Mingoia JP, Squires CG, Stroud RE, Ikonomidis JS. Chronic matrix metalloproteinase inhibition following myocardial infarction in mice: differential effects on short and long-term survival. *J Pharmacol Exp Ther*. 2006;318:966–973.
15. Wilson EM, Moainie SL, Baskin JM, Lowry AS, Deschamps AM, Mukherjee R, Guy TS, St John-Sutton MG, Gorman JH III, Edmunds LH Jr, Gorman RC, Spinale FG. Region- and type-specific induction of matrix metalloproteinases in post-myocardial infarction remodeling. *Circulation*. 2003;107:2857–2863.
16. Huang J, Chen L, Yao Y, Tang C, Ding J, Fu C, Li H, Ma G. Pivotal role of regulator of G-protein signaling 12 in pathological cardiac hypertrophy. *Hypertension*. 2016;67:1228–1236.
17. Chen L, Huang J, Ji YX, Mei F, Wang PX, Deng KQ, Jiang X, Ma G, Li H. Tripartite motif 8 contributes to pathological cardiac hypertrophy through enhancing transforming growth factor beta-activated kinase 1-dependent signaling pathways. *Hypertension*. 2017;69:249–258.
18. Caglayan E, Vantler M, Leppanen O, Gerhardt F, Mustafov L, Ten Freyhaus H, Kappert K, Odenthal M, Zimmermann WH, Tallquist MD, Rosenkranz S. Disruption of platelet-derived growth factor-dependent phosphatidylinositol 3-kinase and phospholipase Cgamma 1 activity abolishes vascular smooth muscle cell proliferation and migration and attenuates neointima formation in vivo. *J Am Coll Cardiol*. 2011;57:2527–2538.
19. Gueguen M, Keuylian Z, Mateo V, Mougenot N, Lompre AM, Michel JB, Meilhac O, Lipskaia L, Limon I. Implication of adenylyl cyclase 8 in pathological smooth muscle cell migration occurring in rat and human vascular remodelling. *J Pathol*. 2010;221:331–342.
20. Lee CS, Kwon YW, Yang HM, Kim SH, Kim TY, Hur J, Park KW, Cho HJ, Kang HJ, Park YB, Kim HS. New mechanism of rosiglitazone to reduce neointimal hyperplasia: activation of glycogen synthase kinase-3beta followed by inhibition of MMP-9. *Arterioscler Thromb Vasc Biol*. 2009;29:472–479.
21. Scott JA, Xie L, Li H, Li W, He JB, Sanders PN, Carter AB, Backs J, Anderson ME, Grumbach IM. The multifunctional Ca2+/calmodulin-dependent kinase II regulates vascular smooth muscle migration through matrix metalloproteinase 9. *Am J Physiol Heart Circ Physiol*. 2012;302:H1953–H1964.
22. Stabile E, Zhou YF, Saji M, Castagna M, Shou M, Kinnaird TD, Baffour R, Ringel MD, Epstein SE, Fuchs S. Akt controls vascular smooth muscle cell proliferation in vitro and in vivo by delaying G1/S exit. *Circ Res*. 2003;93:1059–1065.
23. Zeng L, Li Y, Yang J, Wang G, Margariti A, Xiao Q, Zampetaki A, Yin X, Mayr M, Mori K, Wang W, Hu Y, Xu Q. XBP 1-deficiency abrogates neointimal lesion of injured vessels via cross talk with the PDGF signaling. *Arterioscler Thromb Vasc Biol*. 2015;35:2134–2144.
24. Li M, Feng B, Wang L, Guo S, Zhang P, Gong J, Zhang Y, Zheng A, Li H. Tollip is a critical mediator of cerebral ischaemia-reperfusion injury. *J Pathol*. 2015;237:249–262.
25. Monnerat-Cahli G, Alonso H, Gallego M, Alarcon ML, Bassani RA, Casis O, Medei E. Toll-like receptor 4 activation promotes cardiac arrhythmias by decreasing the transient outward potassium current (Ito) through an IRF3-dependent and MyD88-independent pathway. *J Mol Cell Cardiol*. 2014;76:116–125.
26. Lu C, Ren D, Wang X, Ha T, Liu L, Lee EJ, Hu J, Kalbfleisch J, Gao X, Kao R, Williams D, Li C. Toll-like receptor 3 plays a role in myocardial infarction and ischemia/reperfusion injury. *Biochem Biophys Acta*. 2014;1842:22–31.
27. Yang X, Murthy V, Schultz K, Tatro JB, Fitzgerald KA, Beasley D. Toll-like receptor 3 signaling evokes a proinflammatory and proliferative phenotype in human vascular smooth muscle cells. *Am J Physiol Heart Circ Physiol*. 2006;291:H2334–H2343.
28. Cai Y, Nagel DJ, Zhou Q, Cygnar KD, Zhao H, Li F, Pi X, Knight PA, Yan C. Role of cAMP-phosphodiesterase 1C signaling in regulating growth factor receptor stability, vascular smooth muscle cell growth, migration, and neointimal hyperplasia. *Circ Res*. 2015;116:1120–1132.
29. Owens GK, Kumar MS, Wamhoff BR. Molecular regulation of vascular smooth muscle cell differentiation in development and disease. *Physiol Rev*. 2004;84:767–801.
30. Muto A, Fitzgerald TN, Pimiento JM, Maloney SP, Teso D, Paszkowiak JJ, Westvik TS, Kudo FA, Nishibe T, Dardik A. Smooth muscle cell signal transduction: implications of vascular biology for vascular surgeons. *J Vasc Surg*. 2007;45(suppl A):A15–A24.
31. Chen K, Yuan R, Zhang Y, Geng S, Li L. Tollip deficiency alters atherosclerosis and steatosis by disrupting lipophagy. *J Am Heart Assoc*. 2017;6:e004078. DOI: 10.1161/JAHA.116.004078.
32. Hayashi K, Saga H, Chimori Y, Kimura K, Yamanaka Y, Sobue K. Differentiated phenotype of smooth muscle cells depends on signaling pathways through insulin-like growth factors and phosphatidylinositol 3-kinase. *J Biol Chem*. 1998;273:28860–28867.
33. Hayashi K, Takahashi M, Kimura K, Nishida W, Saga H, Sobue K. Changes in the balance of phosphoinositide 3-kinase/protein kinase B (Akt) and the mitogen-activated protein kinases (ERK/p38MAPK) determine a phenotype of visceral and vascular smooth muscle cells. *J Cell Biol*. 1999;145:727–740.
34. Rzucidlo EM. Signaling pathways regulating vascular smooth muscle cell differentiation. *Vascular*. 2009;17(suppl 1):S15–S20.
35. Fernandez-Hernando C, Jozsef L, Jenkins D, Di Lorenzo A, Sessa WC. Absence of Akt1 reduces vascular smooth muscle cell migration and survival and induces features of plaque vulnerability and cardiac dysfunction during atherosclerosis. *Arterioscler Thromb Vasc Biol*. 2009;29:2033–2040.
36. Martin KA, Merenick BL, Ding M, Fetalvero KM, Rzucidlo EM, Kozul CD, Brown DJ, Chiu HY, Shyu M, Drapeau BL, Wagner RJ, Powell RJ. Rapamycin promotes vascular smooth muscle cell differentiation through insulin receptor substrate-1/phosphatidylinositol 3-kinase/Akt2 feedback signaling. *J Biol Chem*. 2007;282:36112–36120.
37. Xie Y, Jin Y, Merenick BL, Ding M, Fetalvero KM, Wagner RJ, Mai A, Gleim S, Tucker DF, Birnbaum MJ, Ballif BA, Luciano AK, Sessa WC, Rzucidlo EM, Powell RJ, Hou L, Zhao H, Hwa J, Yu J, Martin KA. Phosphorylation of GATA-6 is required for vascular smooth muscle cell differentiation after mTORC1 inhibition. *Sci Signal*. 2015;8:ra44.
38. Aitman TJ, Boone C, Churchill GA, Hengartner MO, Mackay TF, Stemple DL. The future of model organisms in human disease research. *Nat Rev Genet*. 2011;12:575–582.

SUPPLEMENTAL MATERIAL

Table S1.Antibodies for Immunofluorescence

Antibody	Cat No	Manufacturer	Sources of species
Tollip	ab37155	Abcam	Rabbit
PCNA	ab92552	Abcam	Rabbit
CyclinD1	2978	CST	Rabbit
α-SMA	ab7817	Abcam	Mouse
SM22α	ab14106	Abcam	Rabbit
Smoothelin	sc28562	Santa Cruz	Rabbit

Table S2.Primers for real-time PCR

Primer	Sequence(5’ to 3’)
Mmp-9-F	CGGACCCGAAGCGGACAT
Mmp-9-R	GGGGCACCATTTGAGTTT

Table S3.Antibodies for immunoblot analyses.

Antibody	Cat No.	Manufacturer	Sources of species	MW (kDa)
Tollip	ab37155	Abcam	Rabbit	28
PCNA	2586	CST	Mouse	36
CyclinD1	2978	CST	Rabbit	36
MMP9	2270	CST	Rabbit	92
GAPDH	2118	CST	Rabbit	37
α-SMA	ab7817	Abcam	Mouse	43
SM22α	ab28811	Abcam	Mouse	23
Smoothelin	sc28562	Santa Cruz	Rabbit	115
AKT	4691	CST	Rabbit	60
P-AKT	4060	CST	Rabbit	60
GSK3β	9315	CST	Rabbit	46
p-GSK3β	sc130601	Santa Cruz	Rabbit	46
FOXO3A	2497	CST	Rabbit	82-97
P-FOXO3A	9465	CST	Rabbit	97
GAPDH	SC-25778	Santa Cruz	Rabbit	37

Figure S1. The vascular injury-induced Tollip do not derived from endothelial cells

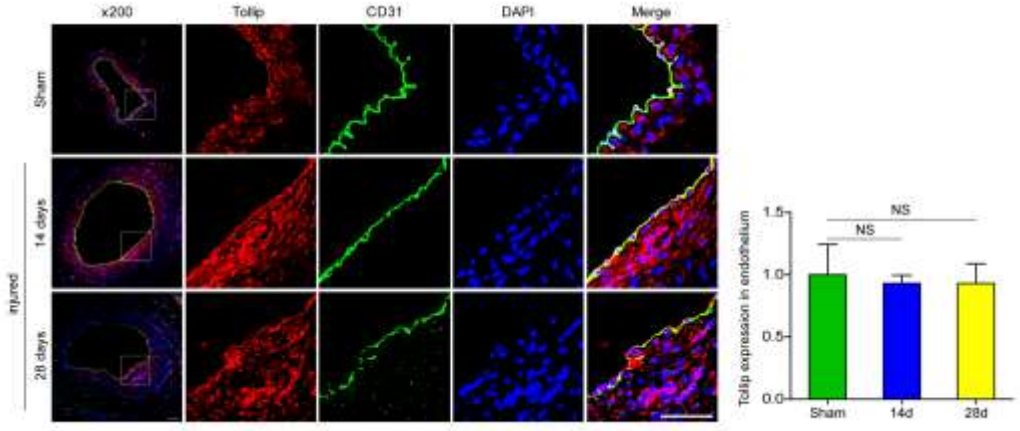

Left: immunofluorescence staining of Tollip (red) and CD31 (green) in the carotid artery sections from WT mice at the indicated times after wire-injury surgery (nucleus stained with DAPI, blue; scale bar, 50 μm). Right: quantitative results of relative Tollip expression in endothelium from the indicated carotid artery sections (n=3each group; N.S. indicates no significant difference).

Figure S2. Tollip expression in SMC-Tollip-TG mice.

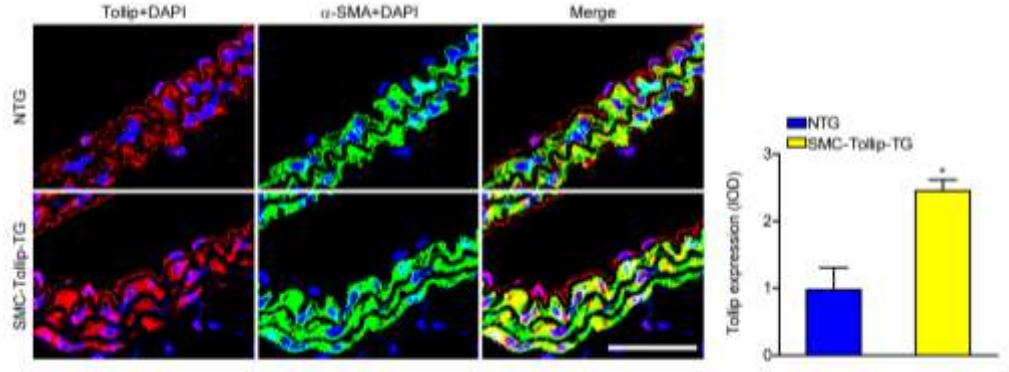

Immunofluorescence staining of Tollip (red) in the carotid arteries from Tollip-TG mice. The arterial smooth muscle cells are indicated by a-SMA (green). DAPI (blue) indicates nuclei. Scale bar=50 μm. The Tollip fluorescence relative OD values are also provided (n = 3 for each group, *P<0.05 vs NTG group).

Figure S3. Tollip neutralizing antibody does not impact VSMC proliferation and dedifferentiation induced by PDGF-BB.

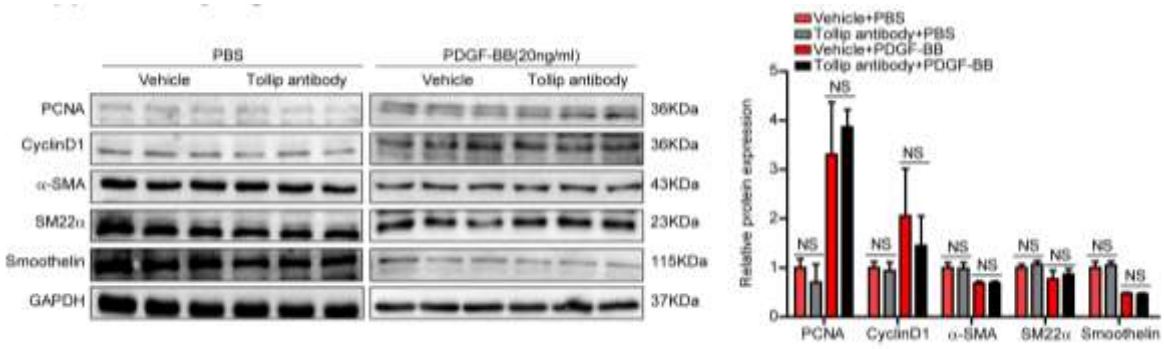

Representative western blots (left) and quantitative results (right) of PCNA, CyclinD1, α-SMA, SM22α and smoothelin protein level in the VSMCs separated from Tollip-TG mice subjected to vehicle or Tollip antibody and treated with PBS or PDGF-BB. (n=3 each group; N.S. indicates no significant difference). GAPDH was used as a loading control in western blot assay.

Figure S4. The phosphorylated AKT expression upon AKT inhibitor treatment.

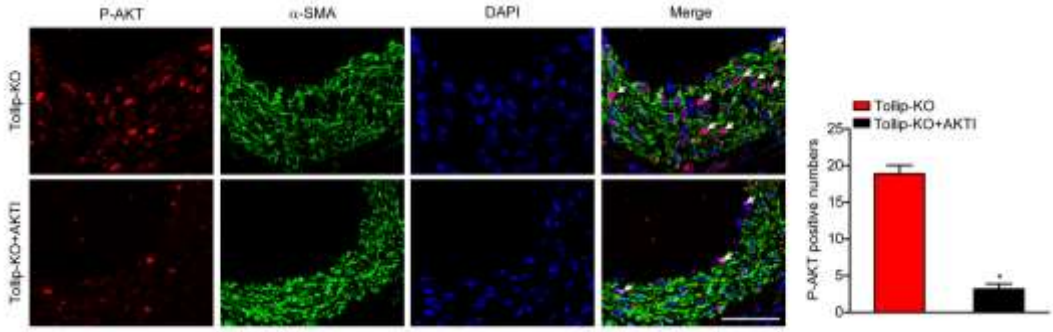

Immunofluorescence staining of the phosphorylated-AKT (red)in the neointima of Tollip-KO mice treated without or with AKT inhibitor after 28 days of wire-injury surgery. The arterial smooth muscle cells are indicated by a-SMA (green). DAPI (blue) indicates nuclei. Scale bar=50 μm.The quantitative results of p-AKT-positive cells are also provided (n = 3 for each group, *P<0.05 vs Tollip-KO group).